III-Sb (001) growth surfaces: structure and island nucleation

W. Barvosa-Carter,* A. S. Bracker, J. C. Culbertson,
B. Z. Nosho, B. V. Shanabrook, and L. J. Whitman
Naval Research Laboratory, Washington DC

Hanchul Kim,[1] N. A. Modine,[1,2] and E. Kaxiras[1]
[1]*Harvard University, Cambridge, MA*
[2]*Sandia National Laboratories, Albuquerque NM*

We have determined the reconstructions present on AlSb and GaSb(001) under conditions typical for device growth by molecular beam epitaxy. Within the range of Sb flux and temperature where the diffraction pattern is nominally (1×3), three distinct (4×3) reconstructions actually occur. The three structures are different than those previously proposed for these growth conditions, with two incorporating *mixed* III-V dimers on the surface. The presence of these hetero-dimers in the top Sb layer leads to an island nucleation and growth mechanism fundamentally different than for other III-V systems.

PACS numbers: 61.16Ch, 68.35.Bs, 73.61.Ey, 81.15.Hi

*Current address: HRL Laboratories, Malibu CA; email: wbc@hrl.com.

11/12/99

DISCLAIMER

DISCLAIMER

Portions of this document may be illegible in electronic image products. Images are produced from the best available original document.

The surface reconstruction on a semiconducting material is the starting point for understanding surface diffusion and the mechanisms of nucleation during growth from the vapor. The steric and energetic landscape across which atoms diffuse is determined by the reconstruction, thus defining the kinetic factors for atomic adsorption and motion, and providing the template for nucleation [1]. These factors are critical to our understanding of homoepitaxial growth and the formation of hetero-interfaces between materials. Semiconductor quantum hetero-structures, for instance, often involve extremely thin layers, and even sub-monolayer variations in layer thickness and interfacial roughness can have dramatic implications for device performance [2,3]. To achieve the level of morphological control needed to optimize the performance of such devices, a detailed understanding of the relevant surface reconstructions and the mechanisms by which epitaxy proceeds is essential.

The role of reconstruction in growth is probably best known for the case of Si(001)-(2×1). Numerous theoretical and experimental studies have shown that monomer and dimer diffusion are highly anisotropic due to the (2×1) reconstruction [4], and that nucleation is strongly influenced by the reconstruction [5]. In comparison, there is a relative dearth of such information for more complex compound semiconducting materials. This deficiency is largely due to the added difficulty of treating the interactions between two (or more) species and a variety of complex non-stoichiometric surface reconstructions. Some recent work using a combination of scanning tunneling microscopy (STM) and kinetic Monte Carlo modeling has begun to elucidate the nucleation and growth mechanisms during molecular beam epitaxy (MBE) of GaAs(001)-(2×4) [6]. However, very little is known about the mechanisms of nucleation and growth for other technologically important III-V semiconductors, such as the antimonides and phosphides.

In this Letter, we present results from a combined experimental and theoretical study where we have determined the structures that occur for a range of Sb-rich growth conditions on AlSb and GaSb. We find that there are two distinct (4×3) reconstructions relevant for typical device growth, and that they both incorporate a novel III-Sb *hetero*-dimer where the group III atom in the dimer is readily available to assist nucleation. For AlSb there is a third (4×3)-like reconstruction where the hetero-dimer is replaced by an Sb dimer, and we show using first-principles calculations that these three reconstructions are the most thermodynamically stable for AlSb. The stability of the hetero-dimer on these surfaces directly determines the mechanism of island nucleation during homoepitaxy.

The AlSb and GaSb surfaces were prepared by MBE and characterized using STM in an interconnected, multichamber ultra-high vacuum facility [7]. The surface reconstructions were studied on *p*-type (Be-doped, 2×10^{16} cm^{-3}), strain-relaxed films (>1 μm thick) grown at 610 °C and 520 °C, respectively, on GaSb(001) substrates. The final 30 ML of each film was left undoped. We obtained sharp reflection high-energy electron diffraction (RHEED) patterns prior to quenching the observed reconstructions in order to maximize the surface order. All STM images were acquired in constant current mode using bias voltages between –3.5 V (filled states) and +2.0 V (empty states) and tunneling currents between 0.03 and 1.0 nA.

The (001) surfaces of the antimonides typically form reconstructions terminated by multiple Sb layers. Under very Sb-rich conditions, AlSb exhibits a c(4×4) reconstruction common to InSb and the arsenides, whereas GaSb reconstructs into metallic (n×5) structures that violate the "electron counting" model (ECM) [8]. Although the structures for these reconstructions have been determined, significant questions remain about the structure of the antimonide surfaces under more typical, less Sb-rich growth conditions. Under such conditions both GaSb and AlSb

exhibit a (1×3)-like RHEED pattern. For GaSb, the (1×3)-like growth conditions have been further delineated by RHEED into distinct c(2×6) and (1×3) (higher temperature/lower Sb flux) regimes [9,10]. Based on analysis of core-level photoemission spectra, simple Sb-dimer models for these structures have been proposed that terminate with 1⅔ monolayers (ML) of Sb and 1⅔ ML Sb + ⅓ ML Ga, respectively (both of which violate the ECM) [10,11]. However, published STM studies suggest the actual (1×3)-like structures are more complex [12,13].

By varying the substrate temperature and Sb_4 flux incident on the surface before quenching, we have discovered that the "(1×3)" phase region for AlSb is in fact composed of three phases that appear at successively lower temperatures and higher Sb_4 fluxes. High-resolution STM images of the different structures are presented in Fig. 1. Following the nomenclature for GaAs, we denote these new phases α(4×3), β(4×3), and γ(4×3) in the order that they are observed under conditions of constant Sb_4 flux and decreasing substrate temperature. The simplest method for forming α(4×3) [Fig. 1(a)] is to anneal the surface near the growth temperature for several minutes without any incident flux. The β structure, shown in Fig. 1(c), is easily stabilized by Sb_4 fluxes typically used during growth. If a β surface is annealed only briefly or under very low Sb flux, a mixture of α and β structures are observed [Fig. 1(b)]. Curiously, although the filled state images for α and β are distinctly different, the empty state images have a similar appearance. The γ phase is only observed under a high Sb_4 flux with the substrate held carefully near the "(1×3)"–to–c(4×4) transition temperature. γ(4×3) can be thought of as a transitional structure between the β and c(4×4) phases, as illustrated in Fig. 1(e) where these three phases are all seen together. It is important to note that surfaces quenched during AlSb epitaxy under typical conditions always exhibit the β reconstruction, even for thin films on InAs substrates [14],

leading us to conclude that this is the reconstruction usually present on the surface during device growth.

The c(4×4)–to–"(1×3)" transition of AlSb(001) is easy to observe using RHEED, however distinguishing between the three (4×3) phases is more difficult. The γ phase shows a weak (4×3) pattern, but it only appears over a narrow temperature-flux range. The α–to–β transition is considerably more difficult to detect using RHEED: the associated changes in the diffraction pattern are limited to subtle intensity changes. Furthermore, the phase transition between α and β appears to be second order, as indicated by the gradual nature of the transition. This is consistent with the STM results, which often show intermixed α+β with no clear phase boundaries. Additionally, on both α and β surfaces there is often considerable disorder with respect to the 4× periodicity.

We find that the α and β(4×3) structures observed on AlSb also occur on GaSb(001), as demonstrated by the striking similarity between the atomic-resolution images of mixed α+β surfaces shown in Fig. 1(b) (AlSb) and 1(d) (GaSb). To date we have not observed the γ phase on GaSb. This is perhaps not surprising given that γ appears to be structurally intermediate between β and c(4×4), and on GaSb the c(4×4) phase is not observed [the unique (*n*×5) phases occur under the corresponding conditions]. We also have preliminary results indicating that similar structures also occur on InSb(001). These observations lead us to suggest that the α(4×3) and β(4×3) reconstructions are probably common to all the antimonides within the range of typical device growth conditions.

To determine the structure of the observed reconstructions and assess their relative stability, we have performed extensive first-principles calculations of the ground-state geometries and

surface energies for a variety of possible structural models, including the previously-proposed (1×3) and c(2×6) structures. The calculations were performed within the local density approximation of density functional theory using the Vienna *Ab initio* Simulation Package [15]. Each reconstructed surface was modeled on a slab of three AlSb bilayers separated by 16 Å of vacuum. The (4×3) surface of the slab was terminated by an additional plane of Sb plus ⅔ ML of surface atoms in dimers, with the opposing surface terminated by fictitious fractionally-charged hydrogen. Atoms were represented using ultrasoft pseudopotentials [16] as supplied by Kresse and Hafner[17]. We used a plane-wave cutoff of 11.5 Ry and k-point sampling equivalent to 144 k-points within the (1×1) surface Brillouin zone. All (4×3) surface atoms and the top two AlSb bilayers were allowed to relax until their rms forces were <0.01 eV/Å. Constant-current STM images were simulated as the height contours of an isosurface of energy-integrated local density of states.

We have confirmed that the structures with the lowest calculated surface energy are the same as those we observe experimentally by comparing the simulated constant-current STM images with the atomic-resolution experimental images. In Fig. 2 we present simulated empty and filled-state images along with structural models for each of the Sb-terminated phases observed on AlSb(001). The correspondence between the experimental and theoretical images is striking – even subtle features such as the relative positions and heights of features seen in the STM images are reproduced. Furthermore, the structure with the lowest calculated surface energy as a function of increasing Sb chemical potential, μ_{Sb}, changes from α to β to γ(4×3) to c(4×4), in direct correspondence with the experimental observations as a function of Sb flux. The excellent agreement between theory and experiment combined with the wide range of structures and experimental conditions explored lead us to conclude that we have identified all

the stable reconstructions that occur under Sb-rich conditions on AlSb(001) (and probably GaSb and InSb as well).

The three (4×3) reconstructions are all structural permutations of the originally-proposed c(2×6) model, which consisted of a full plane of Sb atoms covered by ⅔ ML of Sb in surface dimer rows, each separated by a trench containing rotated dimers in the full plane below. All the (4×3) structures involve the addition of a kink every fourth dimer that moves the dimer by one lattice constant in the [110] direction. Formation of this kink creates two half-filled dangling bonds in the trench that can accept and precisely compensate for the extra electrons that otherwise would cause the c(2×6) to violate the ECM. Although we have not performed tunneling spectroscopy on the (4×3) surfaces of AlSb, based on the calculated band structures, which all exhibit a gap, we would expect them to be semiconducting like the c(4×4) reconstruction [8].

If the Sb flux is high enough, no Al-for-Sb exchange occurs, and the γ(4×3) surface results (1⅔ ML surface Sb, see Fig. 2). However, as the Sb flux is reduced, corresponding to a decrease in μ_{Sb}, the energy is lowered by aligning the Sb dimer rows and replacing one Sb atom in each kink dimer with an Al atom (always the atom between the rows). The resulting β reconstruction is terminated by 1 7/12 ML Sb + 5/12 ML Al. With further decrease in μ_{Sb}, this substitution occurs in the other three top–row dimers and α(4×3) is formed with 1⅓ ML Sb + ⅓ ML Al. Note that this progressive substitution of Al for Sb that occurs as μ_{Sb} decreases is iso-electronic, leaving the surface charge neutrality unchanged.

The III-Sb hetero-dimers undergo an electronic and structural relaxation similar to that observed on III-V (110) surfaces. An electron is transferred between the atoms leaving the Sb

with a filled lone pair and the Al with an empty lone pair. This electron transfer is accompanied by structural relaxation, where the Al relaxes down towards the plane defined by its three Sb neighbors, causing the two Sb neighbors in the layer below to move apart. The resulting structure accounts for the appearance of the hetero-dimers in the STM images: only the Sb filled lone pairs are observed in filled states, but the empty states are a more subtle blend from both the Al atoms and the Sb dimers.

Although transformation between the α and β phases can occur via direct Al/Sb substitution, the β–to–γ and γ–to–c(4×4) transitions are slightly more complex. Strictly speaking, the γ phase actually has a (12×3) conventional unit cell due to the peculiar alignment of the dimers from kink to kink. This symmetry probably arises because the γ phase is structurally constrained between β and c(4×4), giving γ characteristics common to both. However, transforming from γ to either phase requires significant surface rearrangement. Hence, it is possible that the narrow temperature range over which we observe γ is due to a metastable extension of both the β and c(4×4) phase regions into the actual region of γ stability.

To our knowledge, III-V hetero-dimers like those integral to both the α and β(4×3) reconstructions have not been previously observed on a III-V device growth surface [18]. This structure is significant because the group III atom in the mixed dimer is *spatially close to its bulk lattice site*. Generally, the antimonides are distinct from other III-V's because they form (001) reconstructions with multiple Sb layers. As a consequence, the upper Sb layers must be displaced during epitaxial growth. However, because the Al atoms in the hetero-dimers are properly positioned for incorporation into the next layer during growth, *they become natural sites for nucleation.* Moreover, an Al atom deposited on the β(4×3) growth surface can incorporate directly into the lattice via creation of a mixed dimer with very little change in the surface

energy. Such a growth mechanism would be fundamentally different than any observed for the other III-V surfaces.

We have preliminary evidence that these novel (4×3) reconstructions of the III-Sb(001) surfaces in fact play such a role during nucleation and growth. Following sub-monolayer homoepitaxy on AlSb and GaSb, small structures are observed that appear to be the critical nuclei for growth. As shown in Fig. 3, these small structures span two dimer rows and are about two dimers long. Our initial calculations indicate a possible model for these structures that involves six Al atoms supporting two rotated Sb dimers. Although the exact formation process for these critical nuclei is not yet clear, the surrounding reconstruction likely plays a distinct role during subsequent growth. As an island grows, Al incorporates into the surface initially as hetero-dimers in [110]-neighboring (4×3) cells, allowing further Sb dimer adsorption. Larger islands appear to be composed of multiple units of this structure, and when they are large enough, the second-layer dimer row forms on top to make a (disordered) (4×3) reconstructed island. These results further demonstrate the critical role of surface reconstruction in determining the mechanisms of film growth.

We thank B. R. Bennett, M. F. Gyure, F. Grosse, and J. Zinck for helpful discussions, and J. Furthmüller for generating the hydrogen pseudopotentials of fractional charges. This work was supported by the Office of Naval Research and DARPA under the Virtual Integrated Prototyping Initiative.

References

[1] Z. Zhang and M.G. Lagally, Science **276**, 377 (1997), and references therein.

[2] G. Klimeck, R. Lake, and D. K. Blanks, Phys. Rev. B **58**, 7279 (1998).

[3] D. Z.-Y. Ting and T. C. McGill, J. Vac. Sci. Technol. B **14**, 2790 (1996).

[4] Z. Zhang, *et al.*, Phys. Rev. Lett. **74**, 3644 (1995).

[5] B. Voigtländer, *et al.*, Phys. Rev. Lett. **78**, 2164 (1997).

[6] M. Itoh, *et al.*, Phys. Rev. Lett: **81**, 633 (1998).

[7] L. J. Whitman, *et al.*, J. Vac. Sci. Technol. B **14**, 1870 (1996).

[8] L. J. Whitman, *et al.*, Phys. Rev. Lett. **79**, 693 (1997).

[9] J. R. Waterman, B. V. Shanabrook, and R. J. Wagner, J. Vac. Sci. Technol. B **10**, 895 (1992).

[10] M. T. Sieger, T. Miller, and T.-C. Chiang, Phys. Rev. B **52**, 8256 (1995).

[11] G. E. Franklin, *et al.*, Phys. Rev. B **41**, 12619 (1990).

[12] P. M. Thibado, *et al.*, J. Cryst. Growth **175-176**, 317 (1997).

[13] U. Resch-Esser, *et al.*, Phys. Rev. B **55**, 15401 (1997).

[14] B. Z. Nosho *et al.*, J. Vac. Sci. Technol. B **17**, 1786 (1999).

[15] G. Kresse and J. Hafner, Phys. Rev. B **47**, R558 (1994); G. Kresse and J. Furthmüller, Phys. Rev. B **54**, 11169 (1996).

[16] D. Vanderbilt, Phys. Rev. B **41**, 7892 (1990).

[17] G. Kresse and J. Hafner, J. Phys.: Condens. Matter **6**, 8245 (1994).

[18] Structures incorporating mixed III-P dimers have been theoretically predicted for III-rich GaP and InP(001), and there is optical spectroscopy evidence that the structures exist, but it is unknown whether they play any role in epitaxy. See N. Esser *et al.*, J. Vac. Sci. Technol. B **17**, 1691 (1999).

Figure Captions

FIG. 1. (a–c) Filled-state STM images of the "(1×3)" reconstructions observed on AlSb(001) at constant Sb-flux and decreasing temperature. The surface structure evolves from (a) α(4×3), at low or no Sb-flux, through (b) a region of mixed α and β(4×3), to (c) β(4×3) under typical device growth conditions. Empty state images are shown in the insets. (d) The α and β(4×3) as observed on GaSb(001). (e) A quenched mixture of the c(4x4), γ(4×3), and β(4×3) phases on AlSb under high Sb-flux/low temperature conditions. The dashed boxes outline the unit cells.

FIG. 2. Structural models and atomic-scale constant-current images of the stable Sb-rich AlSb(001) reconstructions. (a) A comparison of the experimental (left) and simulated (right) filled-state STM images for α(4×3) (top) and β(4×3) (bottom). Simulated empty-state images are also shown on the right [compare with the insets in Figs. 1(a) and 1(c)]. (b) Simulated images of the γ(4×3) and c(4×4) phases [compare with Fig. 1(e)].

FIG. 3. Filled-state STM image of an AlSb(001)-(4×3) surface following deposition of about 0.2 ML of additional AlSb. A structural model for what appears to be the critical nucleus is shown on the left. A simulated image of this structure is inset on the upper right.

Figure 1
Barvosa-Carter *et al.*

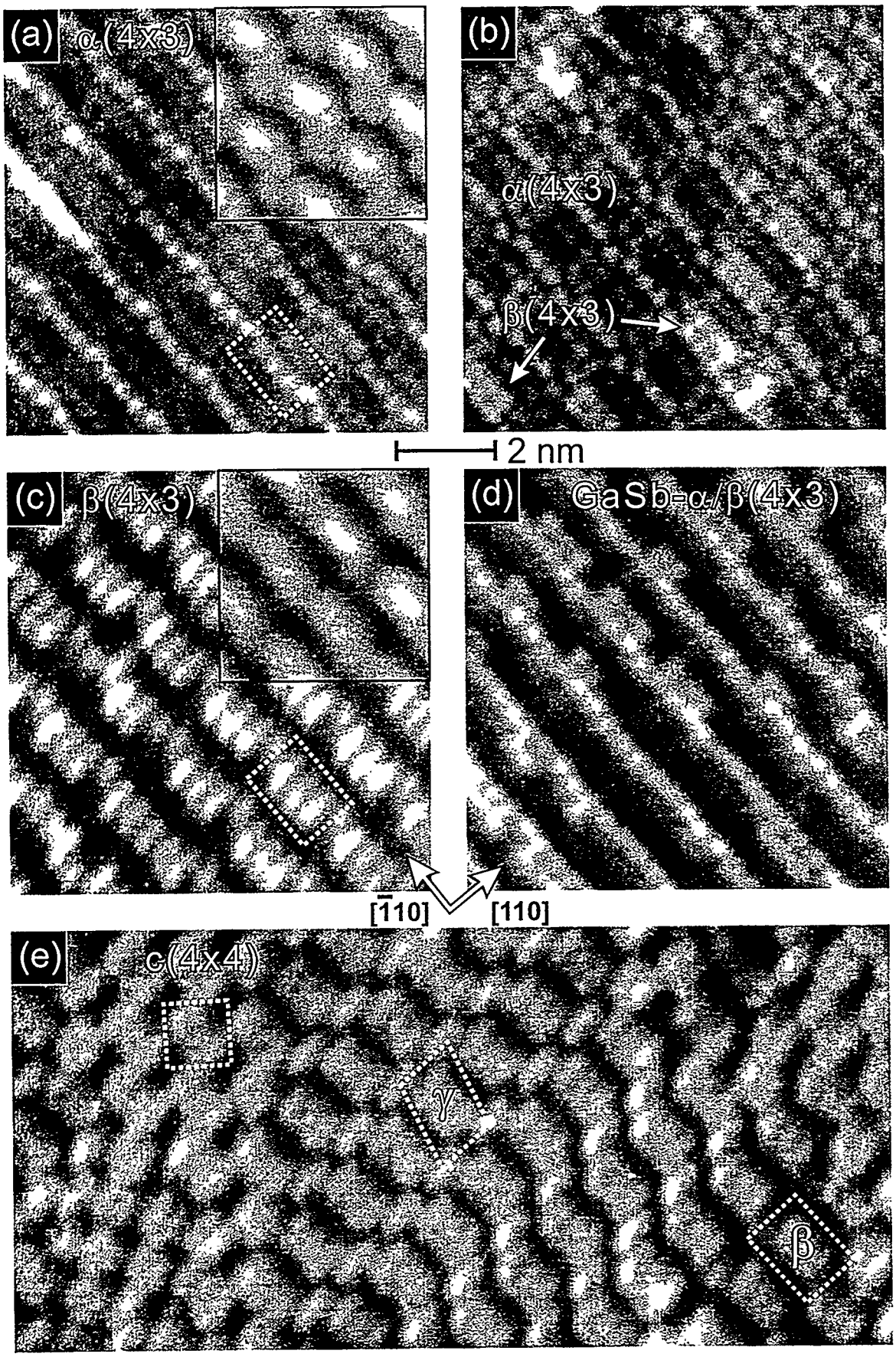

Figure 2
Barvosa-Carter *et al.*

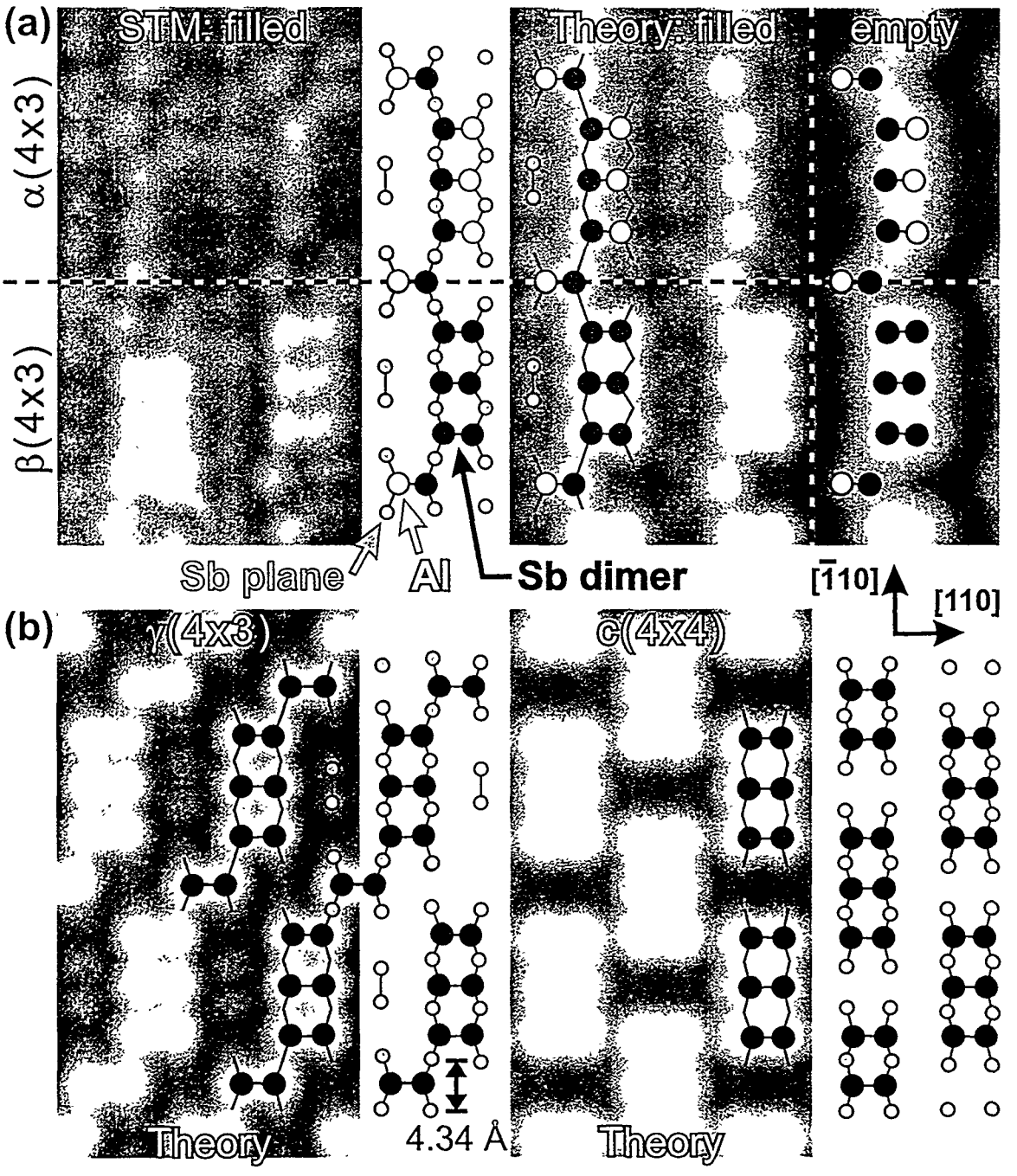

Figure 3
Barvosa-Carter *et al.*